Available online at www.sciencedirect.com
ScienceDirect
Catalysis Today 130 (2008) 80–85
CATALYSIS TODAY
www.elsevier.com/locate/cattod

Support and pretreatment effects on the hydrotreating activity of SBA-15 and CMK-5 supported nickel phosphide catalysts

Tamás I. Korányi [a,*], Zdeněk Vít [b], János B. Nagy [c]

[a] *Chemical Research Center of the Hungarian Academy of Sciences, Budapest, Hungary*
[b] *Institute of Chemical Process Fundamentals, Academy of Sciences of the Czech Republic, Prague, Czech Republic*
[c] *Laboratoire de R.M.N, Facultes Universitaires Notre Dame de la Paix, Namur, Belgium*

Available online 18 October 2007

Abstract

Ni_2P and $Ni_{12}P_5$ containing catalysts were prepared by impregnation of the oxidic precursors on a SBA-15 mesoporous silica or on a CMK-5 nanoporous carbon. Three different kinds of precursors (calcined SBA, not calcined SBA and CMK) were reduced in hydrogen gas stream. X-ray diffraction (XRD) and ^{31}P solid-state nuclear magnetic resonance (NMR) analysis of the passivated catalysts confirmed the presence of Ni_2P and $Ni_{12}P_5$ in all materials prepared from oxidic precursors with initial molar ratio of P/Ni = 2.0 and 0.5, respectively. A mixture of $Ni_{12}P_5$ and Ni_2P was found in the CMK-5 supported catalyst prepared with initial molar ratio of P/Ni = 0.5. Lower HDS and higher HDN steady state reaction rate constants were shown over the SBA-15 supported phosphide catalysts than over a commercial presulfided $NiMo/Al_2O_3$ reference catalyst. The activities with low (P/Ni = 0.5) initial P excess are always higher than those with high (P/Ni = 2) initial P excess. The ratios of HDN over HDS activities are much higher over all phosphide catalysts than over the NiMo reference sample. Higher catalytic activities were found on the silica than on the carbon supported catalysts. The impregnated SBA-15 supported samples were calcined or not before reduction, but it had no effect on the activities. The $Ni_{12}P_5$ containing SBA-15 supported catalysts always exhibited higher hydrotreating activities than the Ni_2P active phase containing ones due to the higher dispersion of the former.

Keywords: Nickel phosphide; SBA-15; CMK-5; Hydrodesulfurization; HDS of thiophene; Hydrodenitrogenation; HDN of pyridine

1. Introduction

Transition-metal phosphides are a novel class of compounds which are promising next-generation hydrotreating catalysts [1]. Bulk transition-metal phosphides [2,3], and silica supported nickel phosphides [3,4] proved to be active hydrodesulfurization (HDS) [5] and hydrodenitrogenation (HDN) [6] catalysts. The silica supported catalysts were prepared by pore-volume impregnation with the appropriate solutions, and after calcination at 623 K the resulting oxidic (metal-phosphate) precursors were reduced in hydrogen flow up to 823 K to metal-phosphides. Precursors with a P-to-Ni ratio of 0.5 yielded mainly $Ni_{12}P_5$. In order to prepare phase-pure silica supported Ni_2P catalysts, an excess of phosphate in the impregnating solution was necessary (P/Ni = 0.65 [4,7], 0.8 [8] or 2 [9]).

New materials of high surface area are necessary to improve catalytic activity and selectivity. Recently other supports than silica like alumina [10], carbon [11,12], MCM-41 [13], and USY [14] are also applied for phosphide catalysts.

The objective of this work is to apply a uniform preparation procedure to obtain $Ni_{12}P_5$ and Ni_2P containing catalysts on new promising ordered mesoporous silica (SBA-15) and carbon (CMK-5) supports and evaluating their activities in simultaneous thiophene HDS and pyridine HDN.

SBA-15 is a mesoporous silica composed of two-dimensionaly hexagonal arrays of uniformly-sized channels with diameters in the range of 5–9 nm [15]. The CMK-5 nanostructured carbon material is formed by using SBA-15 as template, the removal of which leaves 6 nm inside and 9 nm outside uniform diameters ordered graphitic frameworks with a hexagonally packed tubular structure [16,17].

* Corresponding author. Tel.: +36 1 4381100; fax: +36 1 4381143.
E-mail address: koranyi@chemres.hu (T.I. Korányi).

0920-5861/$ – see front matter © 2007 Elsevier B.V. All rights reserved.
doi:10.1016/j.cattod.2007.09.004

We prepared 15–20 wt.% $Ni_{12}P_5$ and Ni_2P containing catalysts on the SBA-15 support with coimpregnation followed by either calcination at 773 K or no calcination, followed by reduction up to 873 K in hydrogen flow and the same catalysts with the same procedure (naturally without calcination) on the CMK-5 support. Three different initial P/Ni ratios (0.5, 0.8 and 2) were used for the preparation of nickel phosphide catalysts.

2. Experimental

The preparation of SBA-15 and CMK-5 supports is given elsewhere [15,16]. Their specific surface areas and pore volumes are 701 and 2000 m^2/g, and 1.17 and 2 ml/g, respectively. The chemicals used for preparation of the catalysts ($Ni(NO_3)_2{\cdot}6H_2O$ (NNA) and $(NH_4)H_2PO_4$ (AHP)) were all Alfa Aesar Puratronic® products with >99.99% purity.

Before catalyst preparations the SBA-15 and CMK-5 supports were dried at 393 K overnight. Appropriate amounts of NNA (0.98 g for 1 g support) and AHP (0.775, 0.310 or 0.194 g for P/Ni = 2, 0.8 or 0.5 ratios for 1 g support) were dissolved in distilled water and mixed in a common metal phosphate solution. The 2 g SBA-15 and 1 g CMK-5 supports were impregnated with the phosphate solutions by the incipient wetness technique. The catalyst precursors were dried at 393 K overnight. The dried sample was pelletized with a press, cracked and sieved to 1.4–0.85 mm size. Half amount of the SBA-15 precursors were heated up with 5 K/min to 773 K in a 1000 ml/min air flow and calcined at this temperature for 3 h, the other half was not calcined. All samples were reduced in a 200 ml/min hydrogen flow. They were heated up in hydrogen to 623 K with 3 K/min, then to 873 K with 1 K/min and kept at this temperature for 1 h, then the gas stream was changed to 2000 ml/min nitrogen and they were taken out from the heating oven and were cooled down to room temperature within 0.5 h. Last the catalysts were passivated with 2000 ml/min nitrogen and 100 ml/min air gas mixture (1 vol% O_2/N_2) for 1 h at room temperature. The catalysts are designated by the support (SBA or CMK), by (C) if calcination was applied, and by the initial P/Ni ratios which were either 2 (high excess phosphorus, H), or 0.8 (excess P, E) or 0.5 (stoichiometric P, S) in the impregnating solutions. A list of the prepared catalysts and their Ni, Mo and P elemental composition (checked by Inductive Coupled Plasma (ICP) measurements) is shown in Table 1.

The X-ray diffractograms (XRD) were obtained on a Philips PW 1050 model with CuK_α radiation. The crystallite size was calculated from the FWHM (Full Width at Half Maximum) values derived from full profile fitting using the Scherrer equation with Warrens correction for instrumental line broadening at $2\Theta = 40^\circ$.

^{31}P NMR spectra were obtained on a Bruker Avance 400 MHz spectrometer at 161.2 MHz. KH_2PO_4 was used to optimize the MAS conditions and also as an external reference (+0.4 ppm relative to 85% H_3PO_4). The samples were placed in a 4 mm rotor and spun at 10 kHz. Spectra were acquired using a single 90 degree P-31 pulse (4 μs) under high-power proton decoupling conditions using composite pulses. The acquisition time varied between 40 and 25 ms, the recycle time was 1 s and 1000–4000 scans were acquired.

Transmission Electron Microscopy (TEM) experiments were carried out in a Philips Tecnai 10 microscope operated at 80–100 kV. The particles were dispersed in ethanol and placed on a carbon grid before TEM examinations.

The catalytic activity was evaluated in parallel HDS of thiophene and HDN of pyridine reactions following pre-reduction in hydrogen stream at 673 K for 2 h in a flow microreactor with fixed catalyst bed over 24–60 mg catalysts at 593 K temperature and 20 bar pressure, as described in detail elsewhere [18,19]. The catalytic activity was determined after 4 h time on stream. All reactions were described by first order kinetic equations derived elsewhere [19]. The rate constants for thiophene HDS (k_{TH}), pyridine hydrogenation (k_{PY}) and piperidine hydrogenolysis (k_{C5}) were calculated by nonlinear regression from the dependences of the molar fractions of components on space time $a_i = f(W/F)$. For comparison purposes the catalytic activity of a commercial NiMo/alumina (Shell 324, 2.8 wt.% Ni, 11.8 wt.% Mo) was evaluated at the same experimental conditions (but instead of reduction, sulfidation with a mixture of 10% H_2S in H_2 was applied), which was reported recently [18].

Table 1
BET specific surface areas, Ni, P contents and molar P/Ni ratios determined by ICP, crystalline phases identified by XRD, ^{31}P NMR signals and crystallite sizes of the passivated phosphide catalyst samples

No.	Sample[a]	S_{BET} (m^2/g)	Ni (wt.%)	P (wt.%)	P/Ni mol ratio	XRD phases	NMR signals	d (nm)[b]
1	$SBA(C)_H$	208	11.0	4.2	0.73	Ni_2P	$Ni_2P + PO_4^{3-}$	11 + 200
2	$SBA(C)_E$	339	11.5	2.8	0.46	Ni_2P	$Ni_2P + PO_4^{3-}$	15
3	$SBA(C)_S$	466	12.1	2.1	0.32	$Ni_{12}P_5$	$Ni_{12}P_5$	20
4	SBA_H	223	11.1	5.2	0.88	Ni_2P	$Ni_2P + PO_4^{3-}$	41
5	SBA_E	364	11.3	2.5	0.42	$Ni_2P + Ni_{12}P_5$	PO_4^{3-}	n.d.[c]
6	SBA_S	454	12.3	2.0	0.31	$Ni_{12}P_5$	$Ni_{12}P_5$	17
7	CMK_H	768	14.8	3.5	0.45	Ni_2P	Ni_2P	20
8	CMK_E	794	15.6	2.5	0.31	Ni_2P	Ni_2P	25
9	CMK_S	809	15.7	3.1	0.38	$Ni_2P + Ni_{12}P_5$	$Ni_2P + Ni_{12}P_5$	25 + 25

[a] SBA, CMK, (C) and subscripts H, E, S refer to SBA-15 supported, CMK-5 supported, calcined catalysts with high excess (H = 2), excess (E = 0.8) and stoichiometric (S = 0.5) initial P/Ni ratios, respectively.
[b] Crystallite size determined by XRD.
[c] Not determined.

3. Results and discussion

All initial P/Ni ratios should be decreased during the catalyst preparation (in the calcination and reduction steps) to the compositions of Ni_2P (P/Ni = 0.5), and $Ni_{12}P_5$ (P/Ni = 0.42), but the $SBA(C)_H$ (P/Ni = 0.73) and SBA_H (P/Ni = 0.88) catalyst samples show definite phosphorus excess, most of the others exhibit P deficiency (Table 1). The composition of the active phase was also checked following the catalytic reaction, but the composition changes remained below 10%.

The powder XRD patterns show the presence of two phosphide phases; Ni_2P and/or $Ni_{12}P_5$ in the passivated catalyst samples (Fig. 1, Table 1). The XRD patterns of the CMK-5 supported catalysts are the most crystalline, the least noisy: CMK_H shows peaks at 40.8, 44.6, 47.3, 54.2, 55.1, and 66.4° and the pattern is similar to a reference pattern for Ni_2P taken from the JCPDS powder diffraction file (card 74–1385), the CMK_S sample contains both phosphide phases in approximately equal amount (Fig. 1). Only Ni_2P phase was detected in the H and E samples with the exception of SBA_E, where some $Ni_{12}P_5$ was also present. Only $Ni_{12}P_5$ phase was identified in the two $SBA(C)_S$ and SBA_S catalysts (Fig. 1, Table 1). Phosphate phases could not be identified in any of the catalysts by XRD. The crystallite sizes calculated by the Scherrer equation are quite uniform, they vary between 15 and 41 nm, except for the $SBA(C)_H$ sample, where due to its sharp cusp like line shape two different crystallite sizes (11 nm and 200 nm) were calculated (Table 1). This indicates that about 85% of the Ni_2P phase is in 11 nm particles and it coexists with 15% of very large (200 nm) Ni_2P crystallites with an average of 25 nm size in the $SBA(C)_H$ sample.

The ^{31}P NMR spectra confirm the presence of crystalline phases identified by XRD and the presence of additional amorphous substances are also be revealed. Ni_2P supported on silica shows two sideband patterns with isotropic chemical shifts at 4081 and 1487 ppm, the shifts for $Ni_{12}P_5$ on SiO_2 are at 2259 and 1941 ppm [4]. Our centre bands are observed at 4074 and 1485–1483 ppm, as well as at 2258 and 1937 ppm in the phosphide NMR spectra of the corresponding samples (Figs. 2 and 3). Accordingly, the phosphide NMR spectra of high excess P containing (H) catalysts contain NMR lines of Ni_2P only (Fig. 2), the spectra of stoichiometric P containing (S) samples possess noisy signals of $Ni_{12}P_5$ at the 1800–2600 ppm chemical shift region (Fig. 3), in agreement with the phases identified by XRD (Table 1). Only the CMK_S sample shows NMR signals of Ni_2P and $Ni_{12}P_5$ species (Table 1, Fig. 3). At least four different phosphate signals with intense signal structures due to paramagnetic phosphates species [20] are presented in the ^{31}P NMR spectra of SBA-15 supported high excess (H) and excess (E) P containing samples between +4 and −40 ppm chemical shifts (not shown), which can be signals of $H_nPO_4^{(3-n)-}$, $P_2O_7^{4-}$, and $(PO_3^-)_n$, respectively [21,22]. The presence of many phosphate species can be the consequence of passivation, which results in the reoxidation of some nickel phosphide particles. Moreover, some unreduced phosphate species [7] are present due to the phosphorus excess in (H) and (E) samples. The NMR spectra of the other catalysts do not present any phosphate signals.

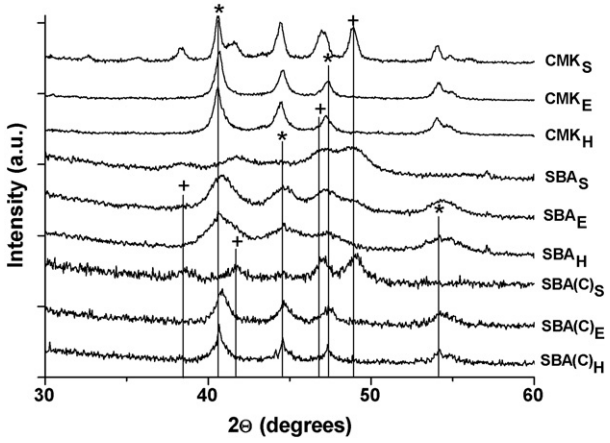

Fig. 1. The XRD patterns of all passivated catalysts. The four most intense lines of Ni_2P and $Ni_{12}P_5$ standards are designated by (*) and (+) symbols, respectively.

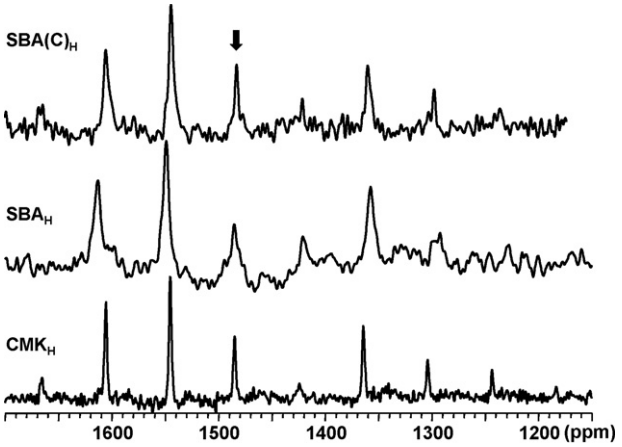

Fig. 2. The Ni_2P region in ^{31}P NMR spectra of high excess (H) P containing $SBA(C)_H$, SBA_H and CMK_H catalysts. The isotropic signal is indicated by an arrow.

The specific surface areas of all catalysts (Table 1) indicate a remarkable decrease compared to the areas of the supports (Section 2). The sorption isotherms (not shown) of SBA-15 supported samples do not present a sharp capillary condensation step, which indicates that some particles are situated inside the mesoporous structure and block some of the pores. These particles can be Ni_2P and phosphate species in the (H) and $Ni_{12}P_5$ in the (S) samples.

Distinct differences in the morphologies and particle sizes of the samples are observed in the TEM micrographs (Fig. 4). The typical pattern of hexagonal SBA-15 structure with a diameter of 8 nm straight pores [23] is clearly seen in the image of $SBA(C)_H$ catalyst (Fig. 4a). The partially ordered graphitic wall structure of CMK-5 support [16] is well seen in Fig. 4c. Particles form aggregates on both kinds of supports. The particle size ranges from approximately 3 to 25 nm similar to the 5–30 nm Ni_2P sizes on silica supports [8,24]. Some nickel phosphide agglomerates are present on the external surface of the support grains (Fig. 4a–d) and some particles seem to be distributed into the support porosity (Fig. 4a and c). Some big

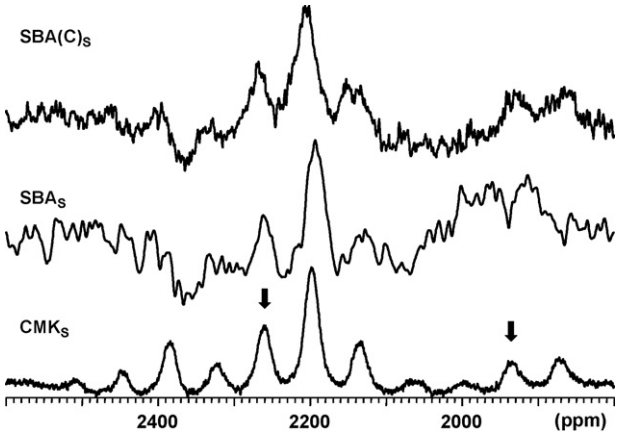

Fig. 3. The $Ni_{12}P_5$ region in ^{31}P NMR spectra of stoichiometric (S) P containing $SBA(C)_S$, SBA_S and CMK_S catalysts. Centerbands are indicated by arrows.

(20–25 nm) particle sizes from the (H) (Fig. 4a and c) and all grain sizes from (S) (Fig. 4b and d) samples with those calculated from XRD (Table 1) resemble each other.

Summarizing the XRD, NMR, BET, and TEM results, the particle size distribution of (H) samples is less homogeneous; therefore they (Ni_2P and phosphate) plug more pores, which results in lower BET specific surface areas than found for (S) samples. The SBA-15 supported (S) catalysts seem to contain two different but homogeneous ($Ni_{12}P_5$) particle size ranges; the large crystallite sizes are seen by XRD (Table 1) and TEM, the small agglomerates reveal themselves in the wide XRD patterns (Fig. 1) and NMR signals (Fig. 3). The CMK_S sample contains both (Ni_2P and $Ni_{12}P_5$) phosphide phases with the large (25 nm) particle sizes only.

The parallel thiophene HDS and pyridine HDN reaction rate constants are summarized in Table 2 for all phosphide catalysts and the reference $NiMo/Al_2O_3$ catalyst. It is well seen that all phosphide catalysts have lower HDS (k_{TH}) activities than for the reference catalyst. All SBA-15 supported samples have similar pyridine hydrogenation (k_{PY}) and generally higher piperidine hydrogenolysis (k_{C5}) activities (reaction rate constants) than that of the reference NiMo catalyst expressed in unit catalyst mass. The HDN activities (k_{PY}, k_{C5}) of CMK-5 supported materials are much lower than their SBA-15 supported counterparts.

The ratio of HDN over HDS activity can be compared by plotting a_{C5} versus a_{C4} (Fig. 5). Apparently it is much higher over the phosphide catalysts than over the NiMo reference sample and the activity ratios of CMK-5 carbon supported catalysts are much lower than those of SBA-15 supported samples (Fig. 5). The presence of Ni_2P and phosphate phases (H and E samples in Table 1) result in relatively low HDN over HDS activity ratios compared to the more homogeneous $Ni_{12}P_5$ phase (S samples in Table 1) similar to the HDS (k_{TH}) and HDN (k_{PY}, k_{C5}) activities over the SBA-15 supported catalysts (Table 2).

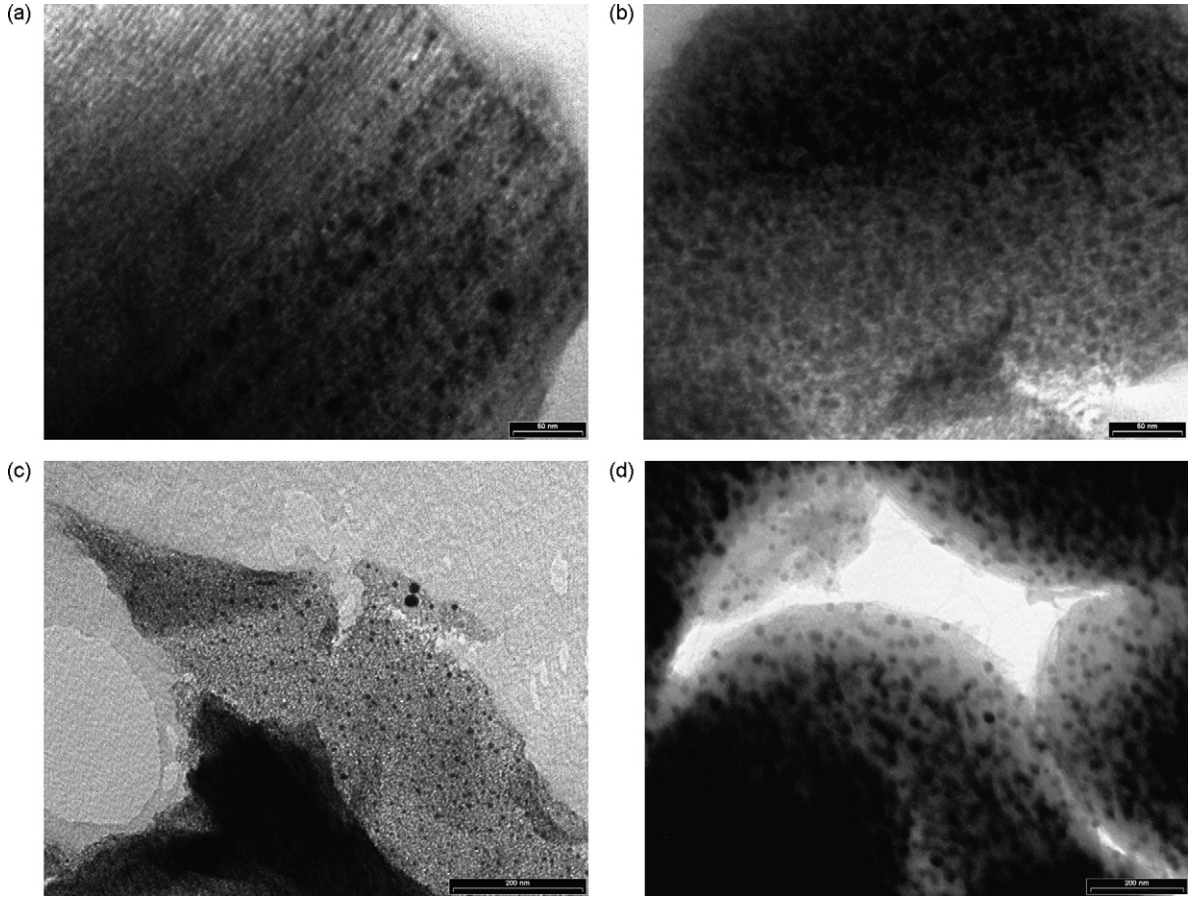

Fig. 4. TEM micrographs of $SBA(C)_H$ (a), $SBA(C)_S$ (b), CMK_H (c), and CMK_S (d) samples.

Table 2
Thiophene HDS (k_{TH}), pyridine hydrogenation (k_{PY}) and piperidine hydrogenolysis (k_{C5}) reaction rate constants in mol/h kg_{cat} units over phosphide and reference catalysts

	$SBA(C)_H$	$SBA(C)_E$	$SBA(C)_S$	SBA_H	SBA_E	SBA_S	CMK_H	CMK_E	CMK_S	NiMo[a]
k_{TH}	1.8	2.3	2.3	1.5	1.6	2.8	1.9	2.5	1.0	8.1
k_{PY}	2.1	2.7	2.8	1.7	2.0	3.2	1.3	0.9	0.4	2.5
k_{C5}	4.9	10.1	19.1	6.9	7.6	29.9	2.8	4.2	1.2	6.1

[a] $NiMo/Al_2O_3$ reference catalyst, data taken from Ref. [18].

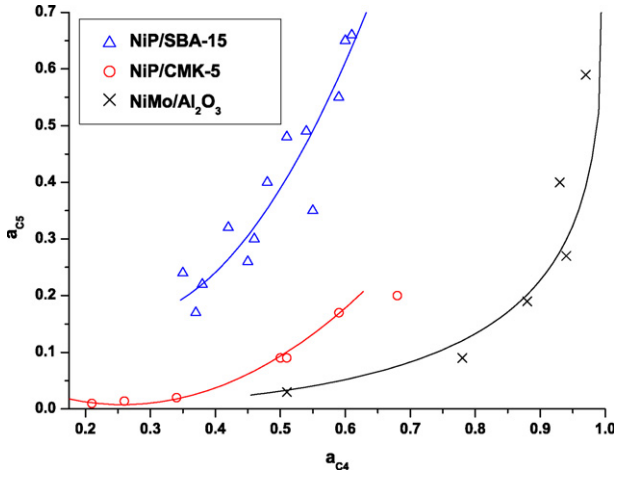

Fig. 5. The ratio of HDN over HDS activity expressed by molar fractions of C_5 hydrocarbons (a_{C5}) plotted versus C_4 hydrocarbons (a_{C4}) over all catalysts.

The number of active surface atoms of SBA_H and SBA_S catalysts was titrated by CO chemisorption. Assuming a stoichiometry of one CO molecule per surface Ni atom, the number of Ni surface atoms was one order of magnitude higher in the SBA_S catalyst compared to the SBA_H sample. Turnover rates cannot be calculated directly from these values, because the residual unreduced phosphate decreases the CO uptake by blocking of CO adsorption sites [9], but the dispersion of SBA_S catalysts is clearly higher than the dispersion of SBA_H catalysts. This dispersion difference can explain the higher activities of the catalysts that only contain $Ni_{12}P_5$ active phase ($SBA(C)_S$ and SBA_S) compared to the activities of Ni_2P and phosphate phase containing (H) samples (Table 1). The activity order is reversed for the CMK-5 supported catalysts (CMK_H is higher than CMK_S, see in Table 2), that is the Ni_2P phase is catalytically more active than the $Ni_{12}P_5$ phase, which is the generally accepted view in the literature [1–14]. The lack of excess phosphate (Table 1), the most crystalline and uniform XRD phases (Fig. 1, Table 1), and the least noisy, therefore the most homogeneous phosphorus containing phases seen by ^{31}P NMR (Figs. 2 and 3) explain this activity order of CMK-5 supported catalysts.

4. Conclusions

The SBA-15 supported catalysts containing only the $Ni_{12}P_5$ active phase (S) always exhibit higher hydrotreating activities than the Ni_2P active phase containing (H) ones. The order of activity is opposite over the carbon supported samples (CMK_H is more active than CMK_S). This different behaviour of the SBA-15 supported catalysts can be due to the inhomogeneous particle size distribution (XRD) or to the plugging of the mesoporous structure (TEM). In addition to that, different phosphates (NMR) are present in the Ni_2P phase containing samples, while the small agglomerates present (XRD, TEM) in the $Ni_{12}P_5$ containing catalysts do not include any phosphate species (NMR). Presumably, the most important effect is the difference in dispersion.

Higher catalytic activities were found on the silica than on the carbon supported catalysts. The calcination before reduction of impregnated SBA-15 supported samples had no effect on the catalytic activities.

The high specific surface area of mesoporous material supports with highly ordered porosity leads to an unusually high piperidine hydrogenolysis activity of SBA-15 supported nickel phosphide catalysts compared to reference $NiMo/Al_2O_3$ sulfide catalysts.

Acknowledgments

The SBA-15 and CMK-5 supports as well as the BET specific surface areas of the catalysts were supplied by the group of Prof. R. Ryoo at KAIST (Korea), which is gratefully acknowledged. The authors wish to thank Dr. I. Sajó (CRC, Hungary) for taking the X-ray diffraction patterns, and Prof. G. Szalontai (Pannon University, Hungary) for recording the NMR spectra. T.I.K. is indebted to F.N.R.S. (Belgium) for financial support. Also, financial support of the work by GA CR (Czech Rep.) through grant No. 104/06/0870 is acknowledged.

References

[1] S. Ted Oyama, J. Catal. 216 (2003) 343.
[2] C. Stinner, R. Prins, Th. Weber, J. Catal. 202 (2001) 187.
[3] V. Zuzaniuk, C. Stinner, R. Prins, Th. Weber, Stud. Surf. Sci. Catal. 143 (2002) 247.
[4] C. Stinner, Z. Tang, M. Haouas, Th. Weber, R. Prins, J. Catal. 208 (2002) 456.
[5] T.I. Korányi, Appl. Catal. A 239 (2003) 253.
[6] W.R.A.M. Robinson, J.N.M. van Gestel, T.I. Korányi, S. Eijsbout, A.M. van der Kraan, J.A.R. van Veen, V.H.J. de Beer, J. Catal. 161 (1996) 539.
[7] V. Zuzaniuk, R. Prins, J. Catal. 219 (2003) 85.
[8] S.J. Sawhill, D.C. Phillips, M.E. Bussell, J. Catal. 215 (2003) 208.
[9] S.T. Oyama, X. Wang, Y.-K. Lee, K. Bando, F. Requejo, J. Catal. 210 (2002) 207.
[10] S.J. Sawhill, K.A. Layman, D.R. van Wyk, M.H. Engelhard, C. Wang, M.E. Bussell, J. Catal. 231 (2005) 300.
[11] Y. Shu, S.T. Oyama, Carbon 43 (2005) 1517.

[12] Y. Shu, S.T. Oyama, Chem. Commun. (2005) 1143.
[13] A. Wang, L. Ruan, Y. Teng, X. Li, M. Lu, J. Ren, Y. Wang, Y. Hu, J. Catal. 229 (2005) 314.
[14] Y.-K. Lee, Y. Shu, S.T. Oyama, Appl. Catal. A 322 (2007) 191.
[15] M. Choi, W. Heo, F. Kleitz, R. Ryoo, Chem. Commun. (2003) 1340.
[16] S.H. Joo, S.J. Choi, I. Oh, J. Kwak, Z. Liu, O. Terasaki, R. Ryoo, Nature 412 (2001) 169.
[17] A.-H. Lu, W.-C. Li, W. Schmidt, W. Kiefer, F. Schüth, Carbon 42 (2004) 2939.
[18] Z. Vít, J. Cinibulk, D. Gulková, Appl. Catal. A 272 (2004) 99.
[19] J. Cinibulk, Z. Vít, Appl. Catal. A 180 (1999) 15.
[20] A. Tuel, L. Canesson, J.C. Volta, Colloid Surf. A 158 (1999) 97.
[21] K. Eichele, R.E. Wasylishen, J. Phys. Chem. 98 (1994) 3108.
[22] G.C. Gunter, R. Craciun, M.S. Tam, J.E. Jackson, D.J. Miller, J. Catal. 164 (1996) 207.
[23] A.H. Janssen, P. van der Voort, A.J. Koster, K.P. de Jong, Chem. Commun. (2002) 1632.
[24] S. Yang, C. Liang, R. Prins, J. Catal. 237 (2006) 118.